THE JOURNAL OF BIOLOGICAL CHEMISTRY VOL. 290, NO. 38, pp. 22945–22954, September 18, 2015

Phosphorylation of Tyrosine 1070 at the GluN2B Subunit Is Regulated by Synaptic Activity and Critical for Surface Expression of *N*-Methyl-D-aspartate (NMDA) Receptors*

Received for publication, May 8, 2015, and in revised form, July 28, 2015 Published, JBC Papers in Press, July 30, 2015, DOI 10.1074/jbc.M115.663450

Wen Lu[‡], Weiqing Fang[‡], Jian Li[‡§], Bin Zhang[‡], Qian Yang[‡], Xunyi Yan[‡], Lin Peng[‡], Heng Ai[¶], Jie-jie Wang[‡], Xiao Liu[‡], Jianhong Luo[‡1], and Wei Yang[‡2]

From the [‡]Department of Neurobiology, Key Laboratory of Medical Neurobiology (Ministry of Health of China), Collaborative Innovation Center for Brain Science, Zhejiang University School of Medicine, Hangzhou, Zhejiang 310058, China, [§]Department of Chemical and Biological Engineering, Zhejiang University, Hangzhou, Zhejiang 310027, China, and [¶]Department of Physiology, Zhejiang Medical College, Hangzhou, Zhejiang 310053, China

Background: *N*-methyl-D-aspartate (NMDA) receptor trafficking is fine-tuned by tyrosine phosphorylation.
Results: Phosphorylation of Tyr-1070 on GluN2B triggers GluN2B-Fyn binding, a process modulated by synaptic activity that up-regulates phosphorylation of Tyr-1472.
Conclusion: Phosphorylation of GluN2B at Tyr-1472 is regulated by a Tyr(P)-1070-mediated association of GluN2B with Fyn.
Significance: This study sheds new light on the surface expression of NMDARs that are implicated in synaptic activity.

The number and subunit composition of synaptic *N*-methyl-D-aspartate receptors (NMDARs) play critical roles in synaptic plasticity, learning, and memory and are implicated in neurological disorders. Tyrosine phosphorylation provides a powerful means of regulating NMDAR function, but the underling mechanism remains elusive. In this study we identified a tyrosine site on the GluN2B subunit, Tyr-1070, which was phosphorylated by a proto-oncogene tyrosine-protein (Fyn) kinase and critical for the surface expression of GluN2B-containing NMDARs. The phosphorylation of GluN2B at Tyr-1070 was required for binding of Fyn kinase to GluN2B, which up-regulated the phosphorylation of GluN2B at Tyr-1472. Moreover, our results revealed that the phosphorylation change of GluN2B at Tyr-1070 accompanied the Tyr-1472 phosphorylation and Fyn associated with GluN2B in synaptic plasticity induced by both chemical and contextual fear learning. Taken together, our findings provide a new mechanism for regulating the surface expression of NMDARs with implications for synaptic plasticity.

N-Methyl-D-aspartate receptors (NMDARs)[3] are ligand-gated ion channels with a high permeability to calcium (1–3) that play critical roles in synaptic plasticity, learning, and memory and neurological disorders (3). Functional NMDARs are thought to be tetramers mainly consisting of two essential GluN1 subunits and two GluN2A-D subunits (2, 4).

NMDAR functions are tightly and finely modulated by the counterbalanced activity of protein-tyrosine kinases and tyrosine phosphatases (5–8). Regulation of NMDARs by phosphorylation is involved in versatile cellular processes, such as channel kinetics, receptor trafficking and location, and protein-protein interactions (9). Previous studies have indicated that inhibition of protein-tyrosine kinase reduces NMDAR currents, whereas inhibition of protein tyrosine phosphatase potentiates them (10). Moreover, accumulating evidence has also shown that Src family kinases such as Fyn and Src are required to up-regulate the tyrosine phosphorylation of NMDARs, further modulating synaptic plasticity and learning and memory (6, 11, 12).

Considering that GluN2B is the predominant tyrosine-phosphorylated protein in the postsynaptic density (PSD) (13), it is important to understand the role of tyrosine phosphorylation in regulating GluN2B function. With the development of mass spectroscopy and phosphorylation-specific antibodies over the last two decades, several tyrosine sites within the carboxyl terminus of the GluN2B subunit have been identified as substrates of Src family kinases (14–16). A major tyrosine site on GluN2B, Tyr-1472, has been reported to control the trafficking of GluN2B-containing NMDARs and may be involved in such processes as synaptic plasticity, memory, and pain (17–20). However, the roles of other tyrosine sites on GluN2B remain to be explored. In the present study we report a novel mechanism by which tyrosine phosphorylation of GluN2B Tyr-1070 (Tyr(P)-1070) facilitates the surface expression of GluN2B-containing NMDARs through its interaction with Fyn and regulating the phosphorylation of GluN2B Tyr-1472 during neuronal activity.

* This work was supported by National Basic Research Program of China Grants 2010CB912002 and 2014CB910300 (to J. Luo) and 2013CB910204 (to W. Y.) and Natural Science Foundation of China Grants 91232303 and 81221003 (to J. Luo) and 30900418 and 81371302 (to W. Y.). The authors declare that they have no conflicts of interest with the contents of this article.
[1] To whom correspondence may be addressed: Dept. of Neurobiology, Zhejiang University School of Medicine, 866 Yu-hang-tang Rd., Hangzhou, Zhejiang 310058, China. Fax: 86-571-88208248; E-mail: luojianhong@zju.edu.cn.
[2] To whom correspondence may be addressed: Dept. of Neurobiology, Zhejiang University School of Medicine, 866 Yu-hang-tang Rd., Hangzhou, Zhejiang 310058, China. Fax: 86-571-88208248. E-mail: yangwei@zju.edu.cn.
[3] The abbreviations used are: NMDAR, *N*-methyl-D-aspartate (NMDA) receptor; PSD, postsynaptic density; co-IP, co-immunoprecipitation; DIV, days *in vitro*; LTP, long term potentiation; cLTP, chemical LTP; cLTD, chemical long term depression; ECS, extracellular solution; CIP, calf intestinal alkaline phosphatase; LV, lentivirus; EGFP, enhanced GFP.

Experimental Procedures

DNA Constructs—pMe-Fyn$_{WT}$ and pMe-Fyn$_{R176K}$ were kind gifts from Tadashi Yamamoto (Okinawa Institute of Science and Technology Graduate University, Kunigami, Okinawa) and were described previously (21). The Y1070F mutant of green fluorescent protein (GFP)-GluN2B (tagged with extracellular amino-terminal GFP) was generated using the QuikChange site-directed mutagenesis kit (Stratagene) following the manufacturer's instructions and verified by DNA sequencing. Western blot, co-immunoprecipitation (co-IP), and subcellular fractionation were performed as described previously (22).

Animals—Fyn knock-out mice were kindly provided by Prof. Yue Feng (Dept. of Pharmacology, Emory University School of Medicine, Atlanta, GA) (23). All experimental procedures were performed in strict accordance with Zhejiang University Animal Experimentation Committee guidelines (the guidelines conform to the National Institutes of Health Guide for the Care and Use of Laboratory Animals). The experiments were approved by the Ethics Committee on Animal Experiments of Zhejiang University. All efforts were made to minimize animal suffering and the number of animals used.

Reagents—Wild-type (WT) GluN1 and GluN2B tagged with extracellular amino-terminal GFP (GFP-GluN2B$_{WT}$) in the pRK5 vector were described previously (24). The primary antibodies used were: Tyr(P)-1472 GluN2B (1:500; Millipore, Lake Placid, NY), mouse GluN2B (1:2000; Cell Signaling, Danvers, MA), Ser(P)-845-GluA1 (1:1000; Millipore), GluA1 (1:1000; Millipore), rabbit monoclonal Fyn (1:2000; Epitomics, Burlingame, CA), mouse monoclonal PSD-95 (1:1000; Abcam, Cambridge, MA), β-actin (1:20000; Sigma), and rabbit monoclonal GFP (1:2000; Epitomics). The secondary antibodies for Western blot were HRP-conjugated, and all were from Thermo Fisher Scientific (Waltham, MA). The secondary antibodies for immunostaining were from Life Technologies. Tetrodotoxin, the Src family kinase inhibitors PP2, PP3, and Su6656, forskolin, and rolipram were all from Tocris Bioscience (Bristol, UK). NMDA, glycine, and picrotoxin were from Sigma.

Generation of Anti-phosphotyrosine 1070 Rabbit Monoclonal Antibody—Anti-phosphotyrosine 1070 rabbit monoclonal antibody was generated using a protocol described previously (25). In brief, New Zealand White rabbits were immunized subcutaneously with 0.2 mg of peptide (ISTHTVTpYGNIEGN, pY is phosphotyrosine) in TiterMax^{TM} Gold Adjuvant (Sigma). After the initial immunization, animals were boosted 3 times at 3-week intervals. Hybridoma fusion was performed according to the established protocol with minor modifications. Hybridoma supernatants were collected and screened for antigen peptide (ISTHTVTpYGNIEGN) and control peptide (ISTHTVTYGNIEGN) by ELISA assays and characterized by immunoblotting using rat brain tissue.

Primary Cortical Cultures—Pregnant Sprague-Dawley rats were killed by cervical dislocation. Briefly, cortical tissues were collected from rats of either sex on embryonic day 18. The tissues were chopped and digested in Hanks' balanced salt solution containing 0.5% trypsin for 10 min at 37 °C. For biochemical analyses, the density of cortical cells was set to 1×10^6/dish in 60-mm dishes precoated overnight with poly-L-lysine. Half of the culture medium was replaced by fresh medium twice per week. The neurons were used at 14–16 days *in vitro* (DIV) unless otherwise noted.

Lentivirus-mediated Knock Down of Fyn—pFUGW-Fyn-shRNA-eGFP lentiviral vector targeted against rat Fyn (5′-GCAGGACAGAAGATGACCT-3′) and EGFP control were from Shanghai GeneChem. Cortical cultures were infected with lentivirus at 7–8 DIV. Seven days after infection, neurons were processed for Western blot analysis.

Treatment of Cortical Cultures—To induce chemical long term potentiation (LTP), we followed a protocol reported previously (26). Briefly, cultures were transferred from Neurobasal medium to extracellular solution (ECS) for the indicated times. The ECS contained 150 mM NaCl, 2 mM $CaCl_2$, 5 mM KCl, 10 mM HEPES, 30 mM glucose, 50 μM forskolin, 0.1 μM rolipram, and 50 μM picrotoxin, pH 7.4. The chemical long term depression (LTD) protocol followed that of a previous study (27). Cortical cultures (14–16 DIV) were incubated with prewarmed extracellular solution (ECS: 150 mM NaCl, 2 mM $CaCl_2$, 5 mM KCl, 10 mM HEPES, 33 mM glucose, 0.5 μM tetrodotoxin, pH 7.4) for 10 min, then 20 μM NMDA and 20 μM glycine were added for the indicated times. Inhibition of Src family kinase activity in cortical cultures was achieved by application of the specific inhibitor PP2 (10 μM) or Su6656 (2 μM). Before drug incubation, the volume of culture medium was adjusted to 2 ml, then the drugs were added to the medium and left for 30 min at 37 °C.

Contextual Fear Conditioning—Behavioral experiments were performed as described with modification (28). Mice were handled for at least 1 week before training. Then they were trained in a near-infrared video fear-conditioning system (Med Associates) with a stainless-steel grid floor. Movement of mice during training was monitored and recorded by a video camera inside the chamber and analyzed using Video Freeze software (Med Associates). During training, each mouse was allowed to freely explore the chambers for 2 min before receiving a 1-s 0.7-mA foot-shock. Subsequently, the mouse received another two foot-shocks at an interval of 1 min. After the foot-shocks, the mouse remained in the chamber for another 1 min before being returned to its home cage. One hour later mice were anesthetized with isoflurane and decapitated. The hippocampi were isolated and immediately stored at −80 °C until use.

Co-IP—The *in vivo* protocol from our previous study was used (22, 29). Co-IP in neuronal culture and HEK293 cells was conducted as described previously (22). Cultured neurons (14–16 DIV) or HEK293 cells were solubilized in modified radioimmune precipitation assay buffer (10 mM Tris, pH 7.4, 150 mM NaCl, 1 mM EDTA, 1% Triton X-100, and 0.25% sodium deoxycholate) with fresh addition of protease and phosphatase inhibitor (1 mM phenylmethylsulfonyl fluoride (PMSF), 1 μg/ml aprotinin, 10 μg/ml leupeptin, 1 mM Na_3VO_4, and 50 mM NaF) at 4 °C for 1 h. The lysates were then centrifuged at 16,000 × *g* at 4 °C for 15 min. The antibodies were mixed with the supernatant after centrifugation at 4 °C for 6 h. After 6 h of incubation of antibody and proteins, ~30 μl of a 50% slurry of Protein A-Sepharose was added to the mixture, and the preparation was further incubated at 4 °C overnight. On the following day the beads were extensively washed in

modified radioimmune precipitation assay buffer and eluted with 2× sample buffer and resolved by SDS-PAGE.

Biotinylation Assay—Biotinylation assays were conducted as reported previously (30, 31).

Subcellular Fractionation—A protocol was adopted from previous reports (32, 33). In brief, the cortex was dissected in cold artificial cerebrospinal fluid and then homogenized in chilled buffer A (0.32 M sucrose and 10 mM HEPES, pH 7.4). The homogenate was centrifuged twice at 1000 × *g* for 10 min. The supernatant was collected and centrifuged again at 12,000 × *g* for 20 min, and the pellet was constituted the crude membrane fraction (P2). The P2 was rinsed with buffer B (4 mM HEPES, 1 mM EDTA, pH 7.4) and centrifuged at 12,000 × *g* for 20 min to precipitate the pellet. The pellet was again rinsed with buffer B and centrifuged again at 12,000 × *g* for 20 min. Afterward, the pellet was incubated with buffer C (20 mM HEPES, 100 mM NaCl, 0.5% Triton X-100, pH 7.2) for 15 min at 4 °C with continuous rotation. Subsequently, the preparation was centrifuged at 12,000 × *g* for 20 min at 4 °C. The supernatant was considered to be the non-postsynaptic density (non-PSD) membrane fraction. The pellet in this step was further solubilized for 1 h at 4 °C with buffer D (20 mM HEPES, 0.15 mM NaCl, 1% Triton X-100, 1% deoxycholic acid, 1% SDS, pH 7.5). Finally, the preparation was centrifuged at 10,000 × *g* for 15 min, and the supernatant was collected and considered to be the PSD membrane fraction. All the above buffers contained protease inhibitors and phosphatase inhibitors.

Western Blot—Western blotting was carried out as described previously (22, 34).

Calf Intestinal Alkaline Phosphatase (CIP) Treatment of Proteins on Nitrocellulose Membrane—About 10 μg of adult male rat hippocampal lysate was subjected to SDS-PAGE. After electrophoresis, the proteins were transferred from gel to nitrocellulose membranes (Hybond-C, GE Healthcare) that were blocked with 5% bovine serum albumin in Tris-buffered saline/Tween 20 for 1 h at room temperature with constant shaking. Next, the membranes were divided into two groups; one was incubated with CIP buffer (100 mM NaCl, 50 mM Tris-HCl, 10 mM $MgCl_2$, 1 mM dithiothreitol, pH 7.9) with fresh addition of protease inhibitor only (1 mM PMSF, 1 μg/ml aprotinin, 10 μg/ml leupeptin), and the other was incubated with CIP and CIP buffer for 1 h at 37 °C. After this step, the membranes were washed three times with Tris-buffered saline/Tween 20 and used for conventional Western blot analysis.

Immunizing Peptide Blocking—Anti-phosphotyrosine 1070 rabbit monoclonal antibody was preincubated with a 2-fold mass excess of the blocking peptide (ISTHTVTpYGNIEGN) for 30 min before immunoblotting. The immunoblotting was conducted as described above.

Immunocytochemistry—Surface-staining of HEK293 cells and cortical neurons was performed as described previously (24). Cortical neurons were plated on coverslips and transfected with the indicated plasmid on DIV 7. On DIV 10, the neurons were rinsed twice in ECS, fixed in 4% paraformaldehyde for 10 min, and then incubated with rabbit GFP primary antibody (1:500) for 15 min at room temperature. After primary antibody application, the neurons were washed 3 times with ECS and incubated with Alexa 546-conjugated secondary antibody (1:500, Invitrogen) for 15 min at room temperature. After three rinses in ECS, the neurons were mounted. Images were captured on the Olympus confocal microscope equipped with a 60×, 1.4 numerical aperture oil-immersion objective using Fluoview 1000. The images were analyzed with ImageJ (NIH, Bethesda, MD). In brief, quantification was performed using the ratio of surface intensity to total intensity. The data from at least three independent experiments are presented as the mean ± S.E.

Whole-cell Patch Clamp Recording—The electrophysiological methods have been described previously (24). The extracellular recording solution contained 147 mM NaCl, 3 mM KCl, 10 mM HEPES, 8 mM glucose, 2 mM $MgCl_2$ (305 mosM, pH adjusted to 7.30 with NaOH). Patch pipettes were filled with an intracellular solution containing 136.5 mM potassium gluconate, 17.5 mM KCl, 9 mM NaCl, 1 mM $MgCl_2$, 10 mM HEPES, 0.2 mM EGTA (300 mosM, pH adjusted to 7.20 with KOH). Recordings were made at −60 mV during the application of 100 μM glutamate and 10 μM glycine to HEK293 cells.

Statistical Analysis—Statistical analysis was performed with Graphpad Prism 5.0 (GraphPad Software, La Jolla, CA). All values are shown as the mean ± S.E. Statistical significance was decided using the two-tailed Student's *t* test for comparing two groups and one-way analysis of variance followed by the post-hoc Bonferroni test for ≥3 groups. The significance level was set at $p \leq 0.05$. * denotes a *p* value of ≤ 0.05; ** denotes a *p* value of ≤ 0.01, and NS indicates a *p* value > 0.05.

Results

GluN2B at the Tyr-1070 Site Is Phosphorylated by Fyn in Vivo and in Vitro—Previous mass spectral analysis has provided evidence that GluN2B is phosphorylated at several tyrosine sites, including Tyr-1070 (15), which lies in the conserved sequence VT*Y*GNI within the carboxyl terminus (Fig. 1*A*). To determine the potential function of Tyr-1070, a rabbit monoclonal antibody was generated and shown to target to the conserved domain around phosphorylated Tyr-1070 (see "Experimental Procedures"). We first verified the specificity of the antibody against Tyr(P)-1070 on GluN2B using CIP assays *in vitro* (35). Our data showed a strong signal of phosphorylated GluN2B by its Tyr(P)-1070 antibody, and phosphatase treatment eliminated this signal (Fig. 1*B*), suggesting that the antibody was phosphorylation-specific. Besides CIP treatment, immunizing peptide blocking experiments also demonstrated that the peptide used for generation of anti-Tyr-1070 antibody completely abolished the immunoreactivity of GluN2B phosphorylated at Tyr-1070 to the antibody, indicating competitive binding of the peptide to the Tyr(P)-1070 antibody (Fig. 1*C*). However, the immunoreactivity of phosphorylated GluN2B at Tyr-1472 was unchanged between the untreated group and the peptide treatment group (Fig. 1, *C* and *D*). Moreover, in the $GluN2B_{Y1070F}$ (tyrosine 1070 to phenylalanine) mutant, the band signal detected by the Tyr(P)-1070 antibody was abolished in GluN2B-expressing HEK293 cells (Fig. 1*E*), confirming that the antibody was Tyr-1070 phosphorylation-specific. Subsequently, the distribution pattern of Tyr(P)-1070 was detected in various rat brain regions, such as the medial prefrontal cortex, hippocampus, amygdala, striatum, and cerebellum (Fig. 1*F*). Our data

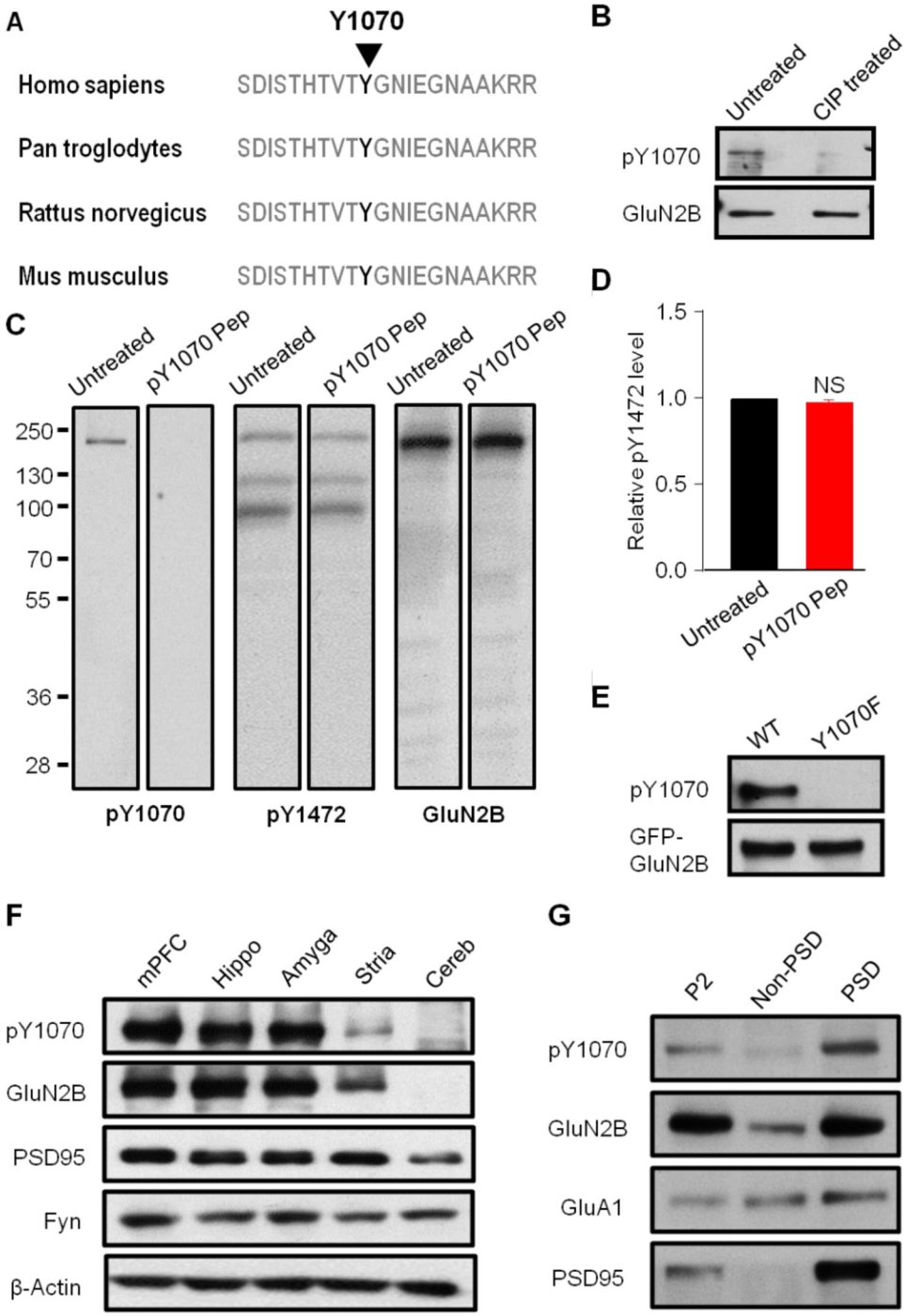

FIGURE 1. **Characterization of a new Tyr-1070 antibody that recognizes the phospho-Tyr-1070 site of GluN2B and determination of the distribution pattern of Tyr(P)-1070 on GluN2B.** *A*, sequence alignment of GluN2B around the Tyr-1070 residue in different species. *B*, representative blots of Tyr(P)-1070 levels in rat cortex lysates with or without CIP treatment ($n = 3$). *C*, representative blots of Tyr(P)-1070, Tyr(P)-1472, and GluN2B levels in cortical neuron lysates with or without Tyr(P)-1070 peptide (*PEP*) treatment ($n = 3$). *D*, quantification of Tyr(P)-1472 levels in *C*. *NS*, no significant difference. *E*, representative blots of Tyr(P)-1070 levels from GluN1/GFP-GluN2B$_{WT}$- and GluN1/GFP-GluN2B$_{Y1070F}$-transfected cells assessed by Tyr-1070-specific antibody ($n = 3$). *F*, representative blots for Tyr(P)-1070, GluN2B, PSD95, and Fyn levels in different brain regions of adult male rat: *mPFC*, medial prefrontal cortex; *Hippo*, hippocampus; *Amyg*, amygdala, *Stria*, striatum; *Cereb*, cerebellum ($n = 3$). *G*, representative blots of Tyr(P)-1070 and Fyn levels in P2, non-PSD, and PSD fractions. Enrichment of PSD95 in the PSD fraction indicates successful separation ($n = 3$).

indicated that the pattern of GluN2B phosphorylated at the Tyr-1070 site (Tyr(P)-1070-GluN2B) was consistent with that of GluN2B *in vivo*, suggesting that it functions broadly throughout the brain. To further determine the subcellular fraction of Tyr(P)-1070 *in vivo*, the P2, non-PSD, and PSD fractions were separated and subjected to Western blot analysis. Our data showed that Tyr(P)-1070-GluN2B was enriched in the PSD fraction compared with the non-PSD fraction (Fig. 1*G*), similar to the distribution pattern of Tyr(P)-1472-GluN2B but not Tyr(P)-1336-GluN2B reported previously (36).

Given that Tyr-1252, Tyr-1336, and Tyr-1472 of GluN2B are phosphorylated by Fyn, to determine whether Tyr-1070 was

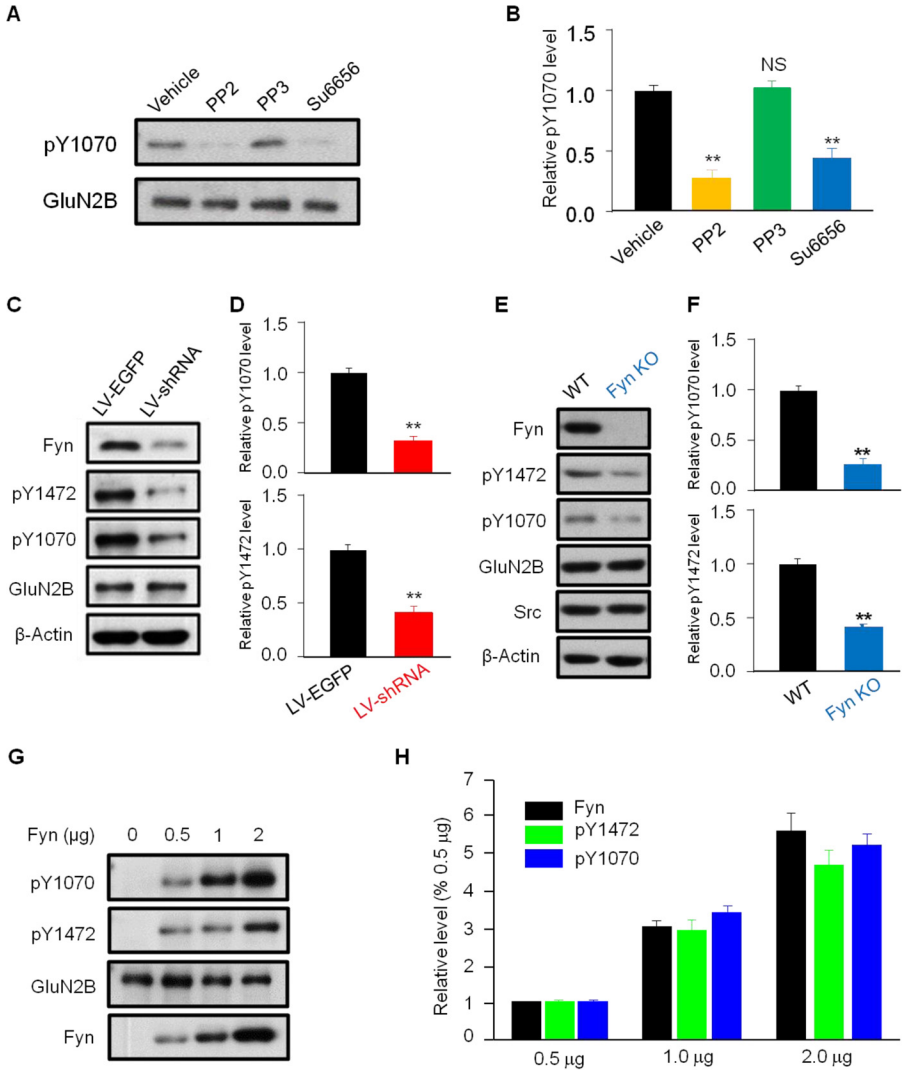

FIGURE 2. **The tyrosine kinase Fyn phosphorylates GluN2B at Tyr-1070.** *A*, the Fyn kinase inhibitors PP2 (10 μM) and Su6656 (2 μM) reduced the Tyr(P)-1070 levels in cultured cortical neurons (DIV 14–16), whereas PP3 did not. *B*, summary data of *panel A* ($n = 4$; **, $p \leq 0.01$; *NS*, no significant difference, one-way analysis of variance). *C*, immunoblotting revealed that lentivirus-mediated Fyn knockdown reduced Tyr(P)-1070 as well as the Tyr(P)-1472 level in cultured cortical neurons. *D*, summary data from C ($n = 4$; **, $p \leq 0.01$, two-tailed *t* test). *E*, immunoblotting revealed that Tyr(P)-1070 and Tyr(P)-1472 levels were significantly reduced in Fyn knock-out mice compared with wild-type mice. *F*, summary data from *E* ($n = 3$ mice/group, **$p \leq 0.01$, two-tailed *t* test). *G*, immunoblotting showed that recombinant Fyn dose-dependently increased the Tyr(P)-1472 and Tyr(P)-1070 levels of GluN2B in transfected HEK293 cells. *H*, summary data from *G*. All data are expressed as the mean ± S.E.

phosphorylated by Fyn, two widely accepted inhibitors of Src family kinases, PP2 and Su6656, were applied to cultured neurons. As expected, the Tyr(P)-1070 level was largely reduced by these inhibitors (27.3 ± 7.1% for PP2, 43.87 ± 8.4% for Su6656, compared with vehicle; Fig. 2, *A* and *B*), but not by PP3, which is a PP2 analog that does not affect Fyn activity (Fig. 2, *A* and *B*), suggesting that Fyn is responsible for regulating the Tyr(P)-1070 level. To confirm this result, we controlled the expression of Fyn in cortical neurons by lentivirus (LV)-Fyn shRNA infection, which significantly reduced Fyn expression (Fig. 2*C*). Accordingly, Tyr(P)-1070 and Tyr(P)-1472 levels were markedly decreased in the LV-Fyn shRNA-treated group (29.6 ± 4.8% of the Tyr(P)-1070 level for LV-shRNA compared with LV-EGFP; 41.3 ± 7.3% of the Tyr(P)-1472 level for LV-shRNA compared with LV-EGFP; Fig. 2, *C* and *D*), but the GluN2B level did not change (100.1 ± 6.1% of the GluN2B level for LV-shRNA compared with LV-EGFP). To further determine whether Fyn is responsible for phosphorylation of GluN2B at the Tyr-1070 site, we then examined the Tyr(P)-1070 and Tyr(P)-1472 levels in the hippocampus from Fyn knock-out and WT mice. Our results showed that both the Tyr(P)-1070 and Tyr(P)-1472 levels were greatly reduced in Fyn knock-out mice compared with WT mice (24.5 ± 7.5% of the Tyr(P)-1070 level and 39.7 ± 2.6% of the Tyr(P)-1472 level, Fyn knock-out *versus* WT; Fig. 2, *E* and *F*), but the GluN2B level did not differ (98.9 ± 7.2% of the GluN2B level, Fyn knock-out *versus* WT). In contrast, the Tyr(P)-1070 level was dramatically boosted and accompanied by a gradual increase of Fyn expression in HEK293 cells (Fig. 2, *G* and *H*). In addition, we noted that the Tyr(P)-1472 level coincided with the Tyr(P)-1070 level during both the inhibition and overexpression of Fyn (Fig. 2, *G* and *H*). Taken together, these results demonstrated that Fyn, a member of the Src kinase family, was responsible for the phosphorylation of Tyr-1070.

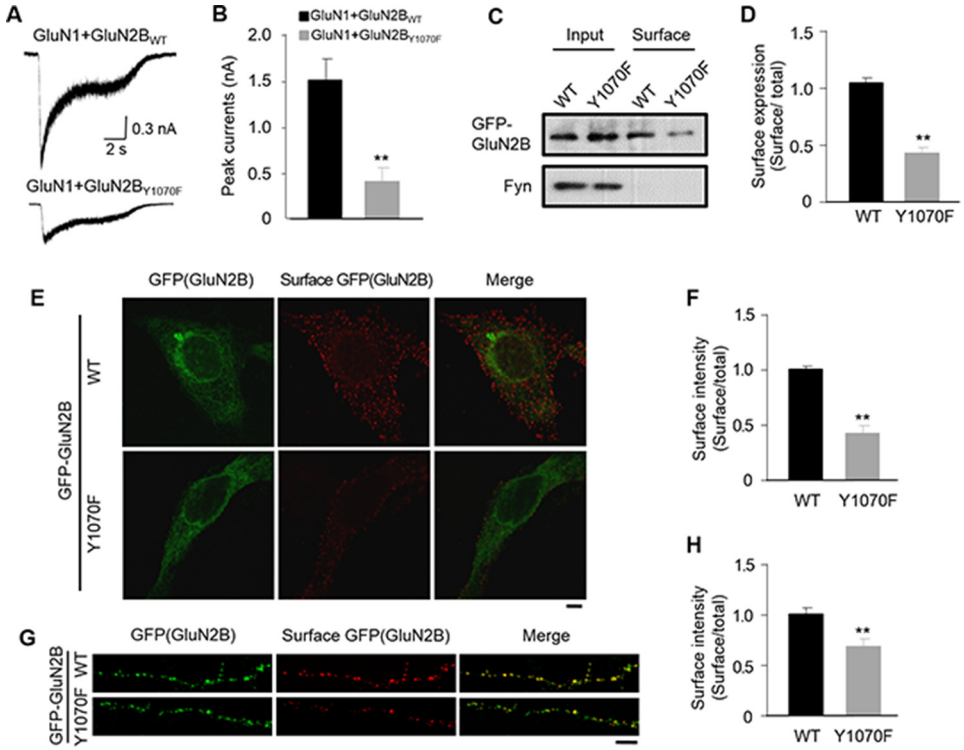

FIGURE 3. **Decreased surface expression in GluN2B Y1070F mutant-transfected HEK293 cells and cultured neurons.** *A*, representative whole-cell currents recorded from HEK293 cells co-transfected with GluN1/GFP-GluN2B$_{WT}$/Fyn or GluN1/GFP-GluN2B$_{Y1070F}$/Fyn. *B*, quantification from *A* ($n = 5$ cells/group; **$p \leq 0.01$ *versus* WT group). *C*, representative immunoblots from biotinylation assays of HEK293 cells co-transfected with GluN1/GFP-GluN2B$_{WT}$/Fyn or GluN1/GFP-GluN2B$_{Y1070F}$/Fyn. *D*, quantification from C ($n = 4$, **, $p \leq 0.01$, two-tailed *t* test). *E*, surface staining of GluN1/GFP-GluN2B/Fyn co-transfected HEK293 cells with anti-GFP antibodies exhibited a significant decrease in cell surface expression of the GFP-GluN2B$_{Y1070F}$ mutant compared with GFP-GluN2B$_{WT}$ (*scale bar*, 20 μm). *F*, quantitative analysis of data from E (300 cells/group from at least three independent experiments; **, $p \leq 0.01$ *versus* WT group, unpaired Student's *t* test). *G*, representative images of surface staining with anti-GFP antibodies in cultured cortical neurons transfected with GFP-GluN2B$_{WT}$ or GluN2B$_{Y1070F}$ (*scale bar*, 5 μm). *H*, quantitative analysis of data as in G (25 neurons/group from five independent cultures; *, $p \leq 0.05$; **, $p \leq 0.01$ *versus* GFP-GluN2B$_{WT}$, two-tailed *t* test).

Decreased Surface Expression of the GluN2B$_{Y1070F}$ Mutant in HEK293 Cells and Neurons—To address whether Tyr-1070 affects the function of NMDARs, we performed whole-cell recording in HEK293 cells transfected with GluN1/GFP-GluN2B$_{WT}$/Fyn or GluN1/GFP-GuN2B$_{Y1070F}$/Fyn. NMDAR current was induced by 100 μM glutamate and 10 μM glycine for 10 s. We found that the amplitude of the NMDAR current in GluN2B$_{Y1070F}$-expressing cells was significantly lower than that of GuN2B$_{WT}$ cells (1488.6 ± 251.16 pA for GFP-GluN2B$_{WT}$, 397 ± 141.1 pA for GFP-GluN2B$_{Y1070F}$, $n = 5$ cells; Fig. 3, *A* and *B*), suggesting that the NMDARs of the GluN2B$_{Y1070F}$ mutant have reduced function. Considering that either surface expression or channel activity determines the NMDAR current, we further used biotinylation assays to clarify this issue. In accordance with the results of electrophysiology, biotinylation assays revealed that the GFP-GluN2B$_{Y1070F}$ mutant had greatly decreased surface expression compared with GFP-GluN2B$_{WT}$ (43.2 ± 4.8% for GFP-GluN2B$_{Y1070F}$ *versus* GluN2B$_{WT}$; Fig. 3, *C* and *D*). To further confirm these results, we visualized the surface NMDARs by surface staining in HEK293 cells (Fig. 3, *E* and *F*). Consistently, the surface expression of GFP-GluN2B$_{WT}$ was much greater than that of GFP-GuN2B$_{Y1070F}$ (Fig. 3*F*). Next, we addressed whether the GluN2B$_{Y1070F}$ mutant also decreased the surface expression of NMDARs in cultured neurons. At DIV 7, GFP-GluN2B$_{WT}$ and the GFP-GluN2B$_{Y1070F}$ mutant were separately transfected into neurons, and surface staining was performed 3 days later. Similar to the results in the heterogeneous system, the surface expression of GluN2B was reduced in GFP-GluN2B$_{Y1070F}$ compared with GFP-GluN2B$_{WT}$-expressing neurons (71.6 ± 3.2% for GFP-GluN2B$_{Y1070F}$ *versus* GluN2B$_{WT}$; Fig. 3, *G* and *H*). Taken together, these findings indicate that Tyr-1070 is critical for the surface expression of GluN2B-containing NMDARs.

Tyr-1070 Regulates the Phosphorylation Level of Tyr-1472 by Mediating the Association of Fyn with GluN2B—By careful analysis of the sequences surrounding Tyr-1070, we found that this site was within a putative immuno-receptor tyrosine-based inhibitory motif that interacts with the SH2 domain of Fyn (37), suggesting that Tyr-1070 mediates the interaction of GluN2B with Fyn. To address this issue, we first determined whether Tyr-1070 is required for GluN2B binding to Fyn. HEK293 cells were separately transfected with plasmids of GluN1/GFP-GluN2B$_{WT}$/Fyn or GluN1/GFP-GluN2B$_{Y1070F}$/Fyn. Our co-IP experiment showed that GFP-GluN2B$_{Y1070F}$ associated much less with Fyn than GFP-GluN2B$_{WT}$ (43.7 ± 4.9% for Y1070F *versus* WT; Fig. 4, *A* and *B*), indicating that Tyr-1070 is a critical site within an SH2-binding immuno-receptor tyrosine-based inhibitory motif. As a control, the association of PSD95 with GluN2B was not significantly changed in GluN2B$_{Y1070F}$ mutant-expressing cells compared with GluN2B$_{WT}$-expressing cells (Fig. 4, *A*, *C*, and *D*).

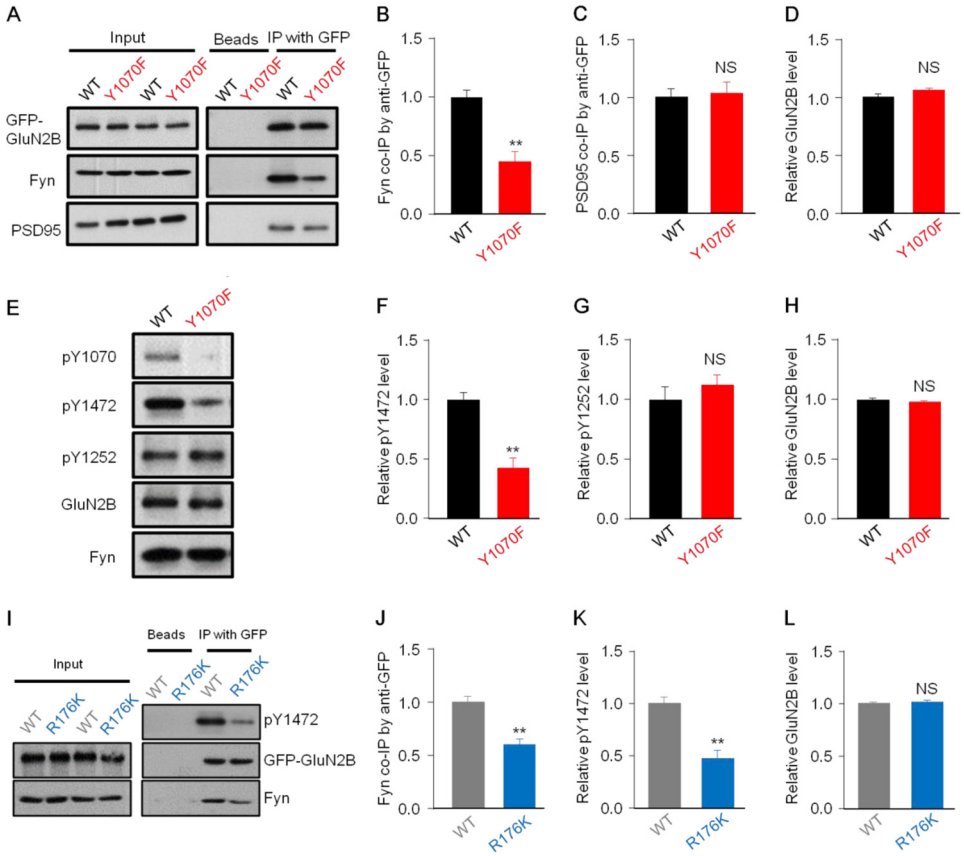

FIGURE 4. **Tyr-1070 is a critical site for GluN2B binding to Fyn and regulating the phosphorylation level of GluN2B at Tyr-1472.** *A–F*, HEK293 cells were co-transfected with GluN1/GFP-GluN2B$_{WT}$/Fyn or GluN1/GFP-GluN2B$_{Y1070F}$/Fyn. *A*, representative co-IP analysis with anti-GFP antibodies showing that remarkably decreased co-IP of Fyn with GluN2B in transfected cells co-expressing the GluN2B$_{Y1070F}$ mutant compared with those co-expressing GluN2B$_{WT}$, but the co-IP of PSD95 and GluN2B exhibited no difference between the two groups. *B–D*, statistical analysis of data from *A* ($n = 7$, **, $p \leq 0.01$, two-tailed *t* test). *NS*, not significant. *E*, representative Western blots of co-transfected cells showing that the phosphorylation level of GluN2B at Tyr-1472, but not at Tyr-1252, was significantly reduced in transfected cells co-expressing the GluN2B$_{Y1070F}$ mutant. *F–H*, quantitative analysis of Tyr(P)-1472, Tyr(P)-1252, and GluN2B levels in GFP-GluN2B$_{WT}$- and GFP-GluN2B$_{Y1070F}$-transfected HEK293 cells ($n = 4$;, **, $p \leq 0.01$, two-tailed *t* test). *I*, HEK293 cells were co-transfected with GluN1/GFP-GluN2B/Fyn$_{WT}$ or GluN1/GFP-GluN2B/Fyn$_{R176K}$, and lysates were subjected to co-IP and immunoblotting. Immunoblotting revealed that the Fyn$_{R176K}$ mutant associated less with GluN2B, and the phosphorylation level of GluN2B Tyr-1472 was lower in transfected cells co-expressing Fyn$_{R176K}$ than in those co-expressing Fyn$_{WT}$. *J–L*, statistical analysis for data as in *F* ($n = 9$; **, $p \leq 0.01$, two-tailed *t* test).

Interestingly, our data showed that the Tyr(P)-1472 level but not the pY1252 level was reduced in the GluN2B$_{Y1070F}$ mutant (42.1 ± 9.6% of the Tyr(P)-1472 level for Y1070F *versus* WT; Fig. 4, *E–G*). As a negative control, the GluN2B level did not change (Fig. 4*H*). Based on these results, we assumed that the Tyr-1070 site mediates the association of GluN2B with Fyn, which specifically regulates the Tyr(P)-1472 level. To determine this issue, we used a single point mutation of Fyn (R176K in the SH2 domain) that disrupted the interaction of Fyn with phosphorylated tyrosine (21). Consistently, our results showed that the interaction between GluN2B and Fyn was decreased in GluN1/GFP-GluN2B/Fyn$_{R176K}$-expressing cells compared with GluN1/GFP-GluN2B/Fyn$_{WT}$-expressing cells (Fig. 4, *I* and *J*). Accordingly, the Tyr(P)-1472 level was also reduced in GluN1/GFP-GluN2B/Fyn$_{R176K}$-expressing cells compared with GluN1/GFP-GluN2B/Fyn-expressing cells (55.3 ± 4.6% for FynR$_{176K}$ *versus* Fyn$_{WT}$; Fig. 4, *I* and *K*), which confirmed that the Tyr(P)-1472 level was dependent on the association of GluN2B with Fyn. As a negative control, the GluN2B level did not change (Fig. 4*L*). Together, these results suggested that Tyr-1070 mediates the association of Fyn with GluN2B, which regulates the Tyr(P)-1472 level.

Both the Phosphorylation of Tyr-1070 on GluN2B and the Interaction of Fyn with GluN2B Are Regulated by Synaptic Activity—Tyr-1472 is finely regulated by synaptic activity, and its phosphorylation is pivotal in preventing the endocytosis of NMDARs, whereas the role of Tyr-1070 in both synaptic activity and learning and memory was unknown. We hypothesized that Tyr-1070 was synchronously regulated with Tyr-1472 by specific synaptic activity. Here, chemical LTP (cLTP) and chemical LTD (cLTD) were used to address this issue in cultured cortical neurons. To induce cLTP, forskolin, rolipram, and picrotoxin were administered to cultured neurons. The phosphorylation level of GluA1 at Ser-845 was dramatically elevated after these stimuli, indicating successful cLTP induction (Fig. 4*A*) as previous reported (38). Interestingly, both the Tyr(P)-1070 and Tyr(P)-1472 levels were markedly increased at 30 min after cLTP stimuli (Fig. 5, *A–C*), but the GluN2B level did not change (Fig. 5*D*). Given that the phosphorylation of Tyr-1472 prevents the endocytosis of NMDARs (18), our results were corroborated by a previous report that such stimuli elevate the surface expression of GluN2B (39).

Opposite to cLTP, cLTD is induced by treating neurons with NMDA and glycine. Successful cLTD was verified by down-

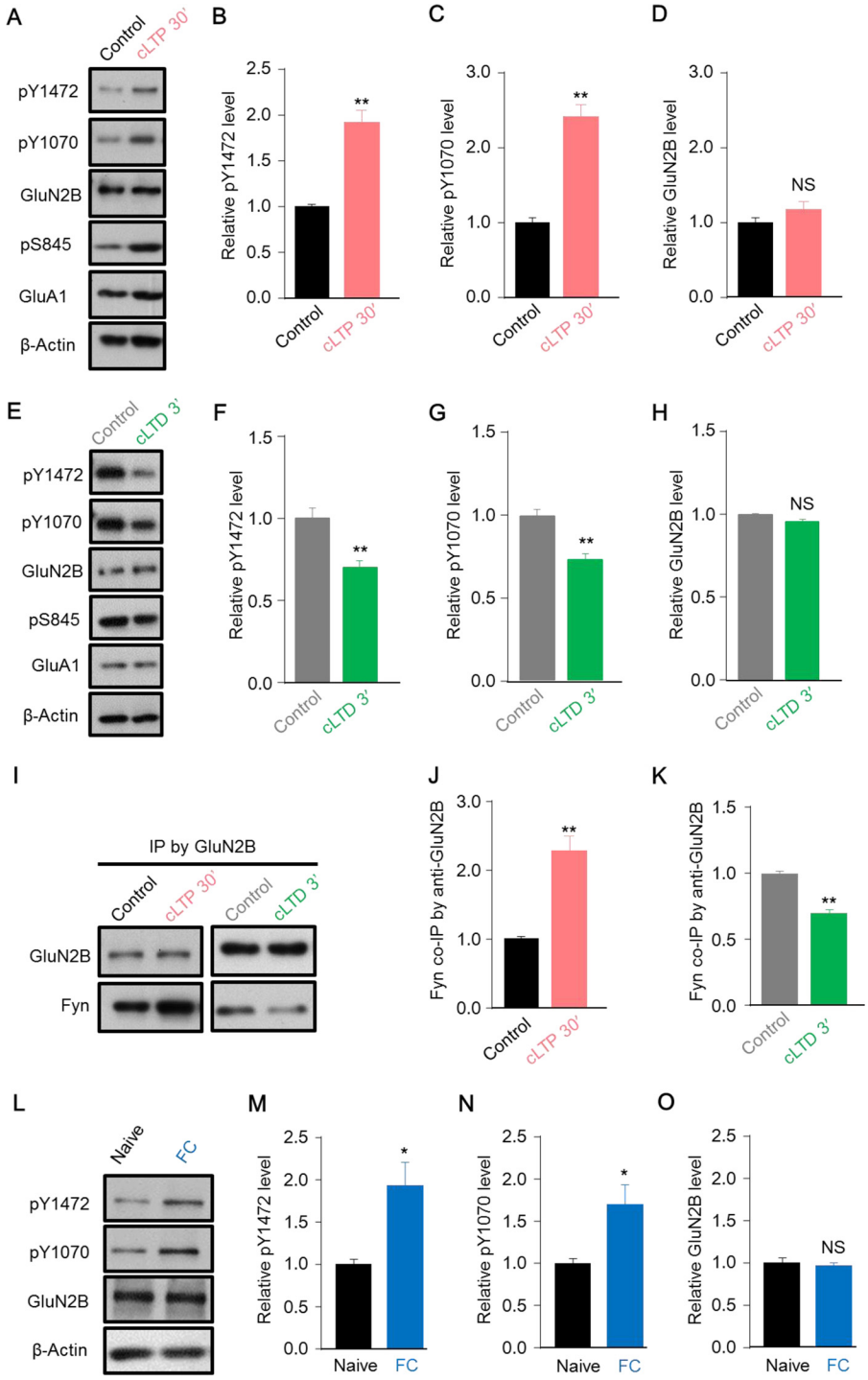

FIGURE 5. **Synaptic activity and contextual fear conditioning regulate the phosphorylation level of GluN2B at Tyr-1070.** *A*, representative blots showing that the cLTP stimuli increased the Ser(P)-845 level of GluA1 as an indicator of successful cLTP and also elevated both the Tyr(P)-1472 and Tyr(P)-1070 levels of GluN2B in cultured cortical neurons (DIV 14–16). *B–D*, quantification of data as in *A* ($n = 4$; **, $p \leq 0.01$, two-tailed *t* test). *NS*, not significant. *E*, representative blots showing that the GluA1 Ser(P)-845 level decreased, and the cLTD stimuli also reduced the GluN2B Tyr(P)-1472 and Tyr(P)-1070 levels in cortical neurons (DIV 14–16). *F–H*, quantification of Tyr(P)-1472, Tyr(P)-1070, and GluN2B levels ($n = 4$; **, $p \leq 0.01$, two-tailed *t* test). *I*, representative blots showing that the cLTP stimuli increased, whereas cLTD decreased, Fyn co-IP with GluN2B. *J*, quantification of Fyn co-IP with GluN2B after LTP stimuli ($n = 4$; **, $p \leq 0.01$, two-tailed *t* test). *K*, quantification of Fyn co-IP with GluN2B after LTD stimuli ($n = 3$; **, $p \leq 0.01$, two-tailed *t* test). *L*, representative blots showing that both the Tyr(P)-1472 and Tyr(P)-1070 levels were increased in hippocampal lysates from mice in the contextual fear conditioning (*FC*) test compared with naïve mice. *M–O*, statistical analysis of data as in J for Tyr(P)-1472, Tyr(P)-1070, and GluN2B levels ($n = 6$ mice; *, $p \leq 0.05$, two-tailed *t* test).

regulating the phosphorylation of GluA1 at Ser-845 (Fig. 5*E*). Our results showed that Tyr(P)-1070 and Tyr(P)-1472 but not GluN2B levels were down-regulated after the induction of cLTD (Fig. 5, *F–H*). Given that the Tyr(P)-1070 and Tyr(P)-1472 levels are bidirectionally regulated by synaptic activity, we assumed that the association of GluN2B with Fyn followed a similar changing pattern in response to cLTP and cLTD stimuli. As expected, cLTP stimuli resulted in a robust increase of

GluN2B association with Fyn (Fig. 5, *I* and *J*). Conversely, cLTD stimuli elicited a dissociation of GluN2B from Fyn (Fig. 4, *I* and *K*). To better understand the function of Tyr-1070 *in vivo*, we further assessed the Tyr(P)-1070 and Tyr(P)-1472 levels in the hippocampus after contextual fear conditioning. Consistently, the Tyr(P)-1070 and Tyr(P)-1472 level in the hippocampus were robustly increased 1 h after conditioning (Fig. 5, *L–N*), but the GluN2B level did not change (Fig. 5*O*), suggesting that the Tyr(P)-1070 level is regulated *in vivo*. Taken together, these findings demonstrate that Tyr(P)-1070 is regulated by synaptic activity both *in vitro* and *in vivo*.

Discussion

The number and composition of synaptic NMDARs are dynamically regulated during development and neuronal activity and thus govern the availability of synaptic plasticity. Therefore, it is important to elucidate the intracellular regulation of NMDAR trafficking. In the present study we demonstrated that Tyr-1070 on GluN2B was a novel Fyn kinase-mediated tyrosine phosphorylation site in response to synaptic activity as well as contextual fear learning. Furthermore, our findings uncovered a new mechanism in which the phosphorylation of GluN2B at Tyr-1472 was regulated by a Tyr(P)-1070-mediated association of GluN2B with Fyn and in turn controlled the surface expression of GluN2B-containing NMDARs.

A previous study reported that Tyr-1252, Tyr-1336, and Tyr-1472 are substrates of Fyn, a member of Src family kinase (15). Here, we identified a new tyrosine site, Tyr-1070, on GluN2B as a substrate of Fyn, which was pivotal for the surface expression of GluN2B-containing NMDARs. Previous studies have shown that site-specific phosphorylation of GluN2B at Tyr-1472, Ser-1480, or Ser-1166 is critical for regulation of the surface expression of NMDARs (8, 18, 40). For example, GluN2B Tyr-1472 is located within an endocytic motif (YEKL), which mediates the interaction of GluN2B with AP-2 and thus facilitates the endocytosis of GluN2B-containing NMDARs (17). Interestingly, we found that Tyr-1070 is a constituent residue of an immunoreceptor tyrosine-based inhibitory motif (VTYGNI) and may indirectly regulate the surface expression of NMDARs. Fyn kinase contains an SH2 domain that is bound to a phosphorylated tyrosine residue, and binding to a phosphorylated tyrosine with its SH2 domain facilitates its activity (6). Although Fyn is in close proximity to NMDARs through association with scaffold proteins such as PSD95 and RACK1 (21, 41), our results showed a direct association of Fyn with GluN2B and that this was regulated by neuronal activity and in turn modulated the Tyr(P)-1472 level. Moreover, our results revealed that changes in the level of Tyr(P)-1070 were coincident with those in Tyr(P)-1472 after cLTP or cLTD stimuli and fear conditioning *in vivo*, suggesting that Tyr-1070 plays a scaffolding role in modulating the Tyr(P)-1472 level and subsequently regulating the surface expression of GluN2B-containing NMDARs. These findings are supported by a study indicating that Src family kinase-mediated phosphorylation of NMDARs stabilizes NMDARs on the cell surface after LTP (42). To our knowledge, the present study provides the first evidence that phosphorylation of one tyrosine site regulates the phosphorylation of another in the GluN2B subunit. In addition, a recent study reported that Ser-1480 on GluN2B is also involved in the modulation of Tyr(P)-1472 levels (43), implying that regulation of Tyr-1472 is complicated. Given multiple tyrosine sites on GluN2B identified to be phosphorylated by Fyn, an intriguing question remaining to be addressed is how the phosphorylation of these sites is differentially regulated by Fyn during specific synaptic activities.

Interestingly, we noted that recent studies have indicated that both Tyr(P)-1070 and Tyr(P)-1472 levels increase after global transient ischemia and reperfusion (16, 44). Besides, a previous study has also revealed that the association of Fyn with NMDARs is enhanced after global transient ischemia (45). By combining this evidence with our findings, we believed that the mechanism of regulating Tyr(P)-1472 via phosphorylated Tyr-1070 is probably also involved in neurological disorders such as ischemic injury (16, 44). In future studies it will be interesting to explore whether manipulation of the Tyr-1070 phosphorylation state and/or the association of GluN2B with Fyn can be targets to ease the damage after ischemic insult.

In summary, we present a new mechanism in which GluN2B phosphorylated at 1070 mediates the interaction of GluN2B with Fyn and subsequently regulates the surface expression of GluN2B-containing NMDARs by modulating the Tyr(P)-1472 level during synaptic activity. Moreover, our findings imply that this mechanism plays a critical role in the functions of NMDARs, which also provide potential therapeutic targets against neurological disorders.

Author Contributions—W. L., W. Y., and J. Luo conceived and designed the experiments and wrote the manuscript. W. L., B. Z., L. P., and H. A. performed the biochemical experiments. W. L. and Q. Y. performed the immunostaining experiments. J. Li made the Tyr(P)-1070 antibody. W. Q. F. performed the fear conditioning test. W. Y. performed the electrophysiological experiments. W. L. and X. Y. Y. analyzed the data; X. L., J.-j. W., and W. L. performed cultured neurons.

Acknowledgment—We thank Dr. Iain C. Bruce for reading the manuscript.

References

1. Cull-Candy, S., Brickley, S., and Farrant, M. (2001) NMDA receptor subunits: diversity, development, and disease. *Curr. Opin. Neurobiol.* **11,** 327–335
2. Prybylowski, K., and Wenthold, R. J. (2004) *N*-methyl-D-aspartate receptors: subunit assembly and trafficking to the synapse. *J. Biol. Chem.* **279,** 9673–9676
3. Lau, C. G., and Zukin, R. S. (2007) NMDA receptor trafficking in synaptic plasticity and neuropsychiatric disorders. *Nat. Rev. Neurosci.* **8,** 413–426
4. Cull-Candy, S. G., and Leszkiewicz, D. N. (2004) Role of distinct NMDA receptor subtypes at central synapses. *Science's STKE 2004,* re16
5. Smart, T. G. (1997) Regulation of excitatory and inhibitory neurotransmitter-gated ion channels by protein phosphorylation. *Curr. Opin. Neurobiol.* **7,** 358–367
6. Salter, M. W., and Kalia, L. V. (2004) Src kinases: a hub for NMDA receptor regulation. *Nat. Rev. Neurosci.* **5,** 317–328
7. Murphy, J. A., Stein, I. S., Lau, C. G., Peixoto, R. T., Aman, T. K., Kaneko, N., Aromolaran, K., Saulnier, J. L., Popescu, G. K., Sabatini, B. L., Hell, J. W., and Zukin, R. S. (2014) Phosphorylation of Ser-1166 on GluN2B by PKA is critical to synaptic NMDA receptor function and Ca^{2+} signaling in spines. *J. Neurosci.* **34,** 869–879

8. Plattner, F., Hernández, A., Kistler, T. M., Pozo, K., Zhong, P., Yuen, E. Y., Tan, C., Hawasli, A. H., Cooke, S. F., Nishi, A., Guo, A., Wiederhold, T., Yan, Z., and Bibb, J. A. (2014) Memory enhancement by targeting Cdk5 regulation of NR2B. *Neuron* **81,** 1070–1083
9. Chen, B. S., and Roche, K. W. (2007) Regulation of NMDA receptors by phosphorylation. *Neuropharmacology* **53,** 362–368
10. Wang, Y. T., and Salter, M. W. (1994) Regulation of NMDA receptors by tyrosine kinases and phosphatases. *Nature* **369,** 233–235
11. Köhr, G., and Seeburg, P. H. (1996) Subtype-specific regulation of recombinant NMDA receptor-channels by protein-tyrosine kinases of the src family. *J. Physiol.* **492,** 445–452
12. Lu, Y. M., Roder, J. C., Davidow, J., and Salter, M. W. (1998) Src activation in the induction of long-term potentiation in CA1 hippocampal neurons. *Science* **279,** 1363–1367
13. Moon, I. S., Apperson, M. L., and Kennedy, M. B. (1994) The major tyrosine-phosphorylated protein in the postsynaptic density fraction is *N*-methyl-D-aspartate receptor subunit 2B. *Proc. Natl. Acad. Sci. U.S.A.* **91,** 3954–3958
14. Ali, D. W., and Salter, M. W. (2001) NMDA receptor regulation by Src kinase signalling in excitatory synaptic transmission and plasticity. *Curr. Opin. Neurobiol.* **11,** 336–342
15. Nakazawa, T., Komai, S., Tezuka, T., Hisatsune, C., Umemori, H., Semba, K., Mishina, M., Manabe, T., and Yamamoto, T. (2001) Characterization of Fyn-mediated tyrosine phosphorylation sites on GluRε2 (NR2B) subunit of the *N*-methyl-D-aspartate receptor. *J. Biol. Chem.* **276,** 693–699
16. Zhang, F., Guo, A., Liu, C., Comb, M., and Hu, B. (2013) Phosphorylation and assembly of glutamate receptors after brain ischemia. *Stroke* **44,** 170–176
17. Lavezzari, G., McCallum, J., Lee, R., and Roche, K. W. (2003) Differential binding of the AP-2 adaptor complex and PSD-95 to the C terminus of the NMDA receptor subunit NR2B regulates surface expression. *Neuropharmacology* **45,** 729–737
18. Prybylowski, K., Chang, K., Sans, N., Kan, L., Vicini, S., and Wenthold, R. J. (2005) The synaptic localization of NR2B-containing NMDA receptors is controlled by interactions with PDZ proteins and AP-2. *Neuron* **47,** 845–857
19. Barki-Harrington, L., Elkobi, A., Tzabary, T., and Rosenblum, K. (2009) Tyrosine phosphorylation of the 2B subunit of the NMDA receptor is necessary for taste memory formation. *J. Neurosci.* **29,** 9219–9226
20. Salter, M. W., and Pitcher, G. M. (2012) Dysregulated Src up-regulation of NMDA receptor activity: a common link in chronic pain and schizophrenia. *FEBS J.* **279,** 2–11
21. Tezuka, T., Umemori, H., Akiyama, T., Nakanishi, S., and Yamamoto, T. (1999) PSD-95 promotes Fyn-mediated tyrosine phosphorylation of the *N*-methyl-D-aspartate receptor subunit NR2A. *Proc. Natl. Acad. Sci. U.S.A.* **96,** 435–440
22. Wang, Y. B., Wang, J. J., Wang, S. H., Liu, S. S., Cao, J. Y., Li, X. M., Qiu, S., and Luo, J. H. (2012) Adaptor protein APPL1 couples synaptic NMDA receptor with neuronal prosurvival phosphatidylinositol 3-kinase/Akt pathway. *J. Neurosci.* **32,** 11919–11929
23. Lu, Z., Ku, L., Chen, Y., and Feng, Y. (2005) Developmental abnormalities of myelin basic protein expression in fyn knock-out brain reveal a role of Fyn in posttranscriptional regulation. *J. Biol. Chem.* **280,** 389–395
24. Yang, W., Zheng, C., Song, Q., Yang, X., Qiu, S., Liu, C., Chen, Z., Duan, S., and Luo, J. (2007) A three amino acid tail following the TM4 region of the *N*-methyl-D-aspartate receptor (NR) 2 subunits is sufficient to overcome endoplasmic reticulum retention of NR1–1a subunit. *J. Biol. Chem.* **282,** 9269–9278
25. Spieker-Polet, H., Sethupathi, P., Yam, P. C., and Knight, K. L. (1995) Rabbit monoclonal antibodies: generating a fusion partner to produce rabbit-rabbit hybridomas. *Proc. Natl. Acad. Sci. U.S.A.* **92,** 9348–9352
26. Szepesi, Z., Bijata, M., Ruszczycki, B., Kaczmarek, L., and Wlodarczyk, J. (2013) Matrix metalloproteinases regulate the formation of dendritic spine head protrusions during chemically induced long-term potentiation. *PloS ONE* **8,** e63314
27. Behnisch, T., Yuanxiang, P., Bethge, P., Parvez, S., Chen, Y., Yu, J., Karpova, A., Frey, J. U., Mikhaylova, M., and Kreutz, M. R. (2011) Nuclear translocation of jacob in hippocampal neurons after stimuli inducing long-term potentiation but not long-term depression. *PloS ONE* **6,** e17276
28. Fowler, S. W., Chiang, A. C., Savjani, R. R., Larson, M. E., Sherman, M. A., Schuler, D. R., Cirrito, J. R., Lesné, S. E., and Jankowsky, J. L. (2014) Genetic modulation of soluble Abeta rescues cognitive and synaptic impairment in a mouse model of Alzheimer's disease. *J. Neurosci.* **34,** 7871–7885
29. Luo, J., Wang, Y., Yasuda, R. P., Dunah, A. W., and Wolfe, B. B. (1997) The majority of *N*-methyl-D-aspartate receptor complexes in adult rat cerebral cortex contain at least three different subunits (NR1/NR2A/NR2B). *Mol. Pharmacol.* **51,** 79–86
30. Cao, M., Xu, J., Shen, C., Kam, C., Huganir, R. L., and Xia, J. (2007) PICK1-ICA69 heteromeric BAR domain complex regulates synaptic targeting and surface expression of AMPA receptors. *J. Neurosci.* **27,** 12945–12956
31. Lu, W., Ai, H., Peng, L., Wang, J. J., Zhang, B., Liu, X., and Luo, J. H. (2015) A novel phosphorylation site of *N*-methyl-D-aspartate receptor GluN2B at S1284 is regulated by Cdk5 in neuronal ischemia. *Exp. Neurol.* **271,** 251–258
32. Pacchioni, A. M., Vallone, J., Worley, P. F., and Kalivas, P. W. (2009) Neuronal pentraxins modulate cocaine-induced neuroadaptations. *J. Pharmacol. Exp. Ther.* **328,** 183–192
33. Milnerwood, A. J., Gladding, C. M., Pouladi, M. A., Kaufman, A. M., Hines, R. M., Boyd, J. D., Ko, R. W., Vasuta, O. C., Graham, R. K., Hayden, M. R., Murphy, T. H., and Raymond, L. A. (2010) Early increase in extrasynaptic NMDA receptor signaling and expression contributes to phenotype onset in Huntington's disease mice. *Neuron* **65,** 178–190
34. Ai, H., Yang, W., Ye, M., Lu, W., Yao, L., and Luo, J. H. (2011) Differential regulation of AMPA receptor GluA1 phosphorylation at serine 831 and 845 associated with activation of NMDA receptor subpopulations. *Neurosci. Lett.* **497,** 94–98
35. Kornhauser, J. M., Cowan, C. W., Shaywitz, A. J., Dolmetsch, R. E., Griffith, E. C., Hu, L. S., Haddad, C., Xia, Z., and Greenberg, M. E. (2002) CREB transcriptional activity in neurons is regulated by multiple, calcium-specific phosphorylation events. *Neuron* **34,** 221–233
36. Goebel-Goody, S. M., Davies, K. D., Alvestad Linger, R. M., Freund, R. K., and Browning, M. D. (2009) Phospho-regulation of synaptic and extrasynaptic *N*-methyl-D-aspartate receptors in adult hippocampal slices. *Neuroscience* **158,** 1446–1459
37. Daëron, M., Jaeger, S., Du Pasquier, L., and Vivier, E. (2008) Immunoreceptor tyrosine-based inhibition motifs: a quest in the past and future. *Immunol. Rev.* **224,** 11–43
38. Boehm, J., Kang, M. G., Johnson, R. C., Esteban, J., Huganir, R. L., and Malinow, R. (2006) Synaptic incorporation of AMPA receptors during LTP is controlled by a PKC phosphorylation site on GluR1. *Neuron* **51,** 213–225
39. Qiu, S., Chen, T., Koga, K., Guo, Y. Y., Xu, H., Song, Q., Wang, J. J., Descalzi, G., Kaang, B. K., Luo, J. H., Zhuo, M., and Zhao, M. G. (2013) An increase in synaptic NMDA receptors in the insular cortex contributes to neuropathic pain. *Sci. Signal.* **6,** ra34
40. Chung, H. J., Huang, Y. H., Lau, L. F., and Huganir, R. L. (2004) Regulation of the NMDA receptor complex and trafficking by activity-dependent phosphorylation of the NR2B subunit PDZ ligand. *J. Neurosci.* **24,** 10248–10259
41. Yaka, R., Thornton, C., Vagts, A. J., Phamluong, K., Bonci, A., and Ron, D. (2002) NMDA receptor function is regulated by the inhibitory scaffolding protein, RACK1. *Proc. Natl. Acad. Sci. U.S.A.* **99,** 5710–5715
42. Grosshans, D. R., Clayton, D. A., Coultrap, S. J., and Browning, M. D. (2002) LTP leads to rapid surface expression of NMDA but not AMPA receptors in adult rat CA1. *Nat. Neurosci.* **5,** 27–33
43. Sanz-Clemente, A., Matta, J. A., Isaac, J. T., and Roche, K. W. (2010) Casein kinase 2 regulates the NR2 subunit composition of synaptic NMDA receptors. *Neuron* **67,** 984–996
44. Knox, R., Brennan-Minnella, A. M., Lu, F., Yang, D., Nakazawa, T., Yamamoto, T., Swanson, R. A., Ferriero, D. M., and Jiang, X. (2014) NR2B phosphorylation at tyrosine 1472 contributes to brain injury in a rodent model of neonatal hypoxia-ischemia. *Stroke* **45,** 3040–3047
45. Takagi, N., Cheung, H. H., Bissoon, N., Teves, L., Wallace, M. C., and Gurd, J. W. (1999) The effect of transient global ischemia on the interaction of Src and Fyn with the *N*-methyl-D-aspartate receptor and postsynaptic densities: possible involvement of Src homology 2 domains. *J. Cereb. Blood Flow Metab.* **19,** 880–888